JEM

Supplemental material

Roussel et al., **https://doi.org/10.1084/jem.20180668**

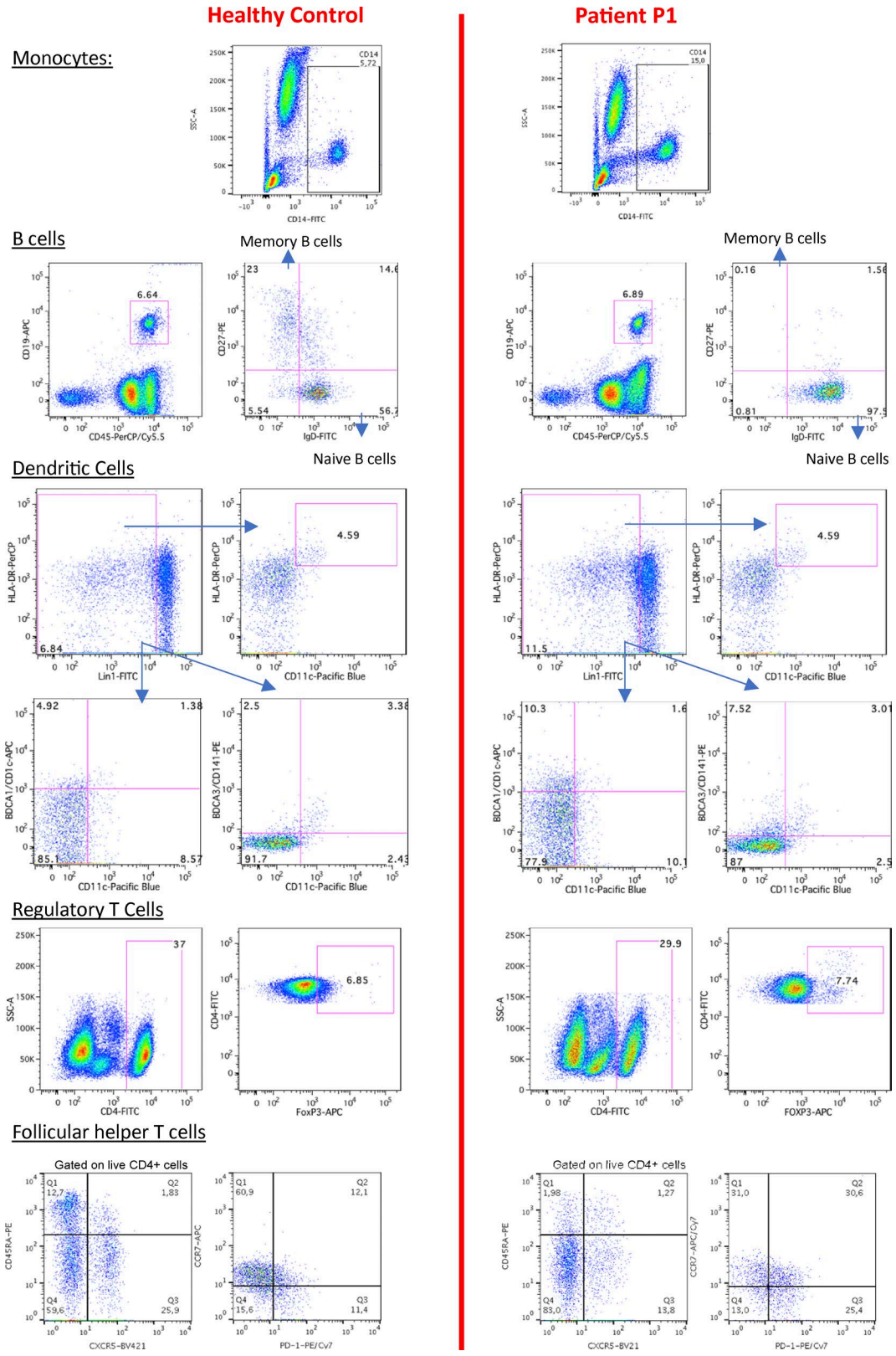

Figure S1. **Flow cytometry gating strategy on whole blood or peripheral blood mononuclear cells from HC or P1.** Cells were gated on the basis of their FSC-A/SSC-a, singlets cells (FSC-A, FSC-H), live cells, and target population (monocytes, B cells, DCs, regulatory T cells, and Tfh cells).

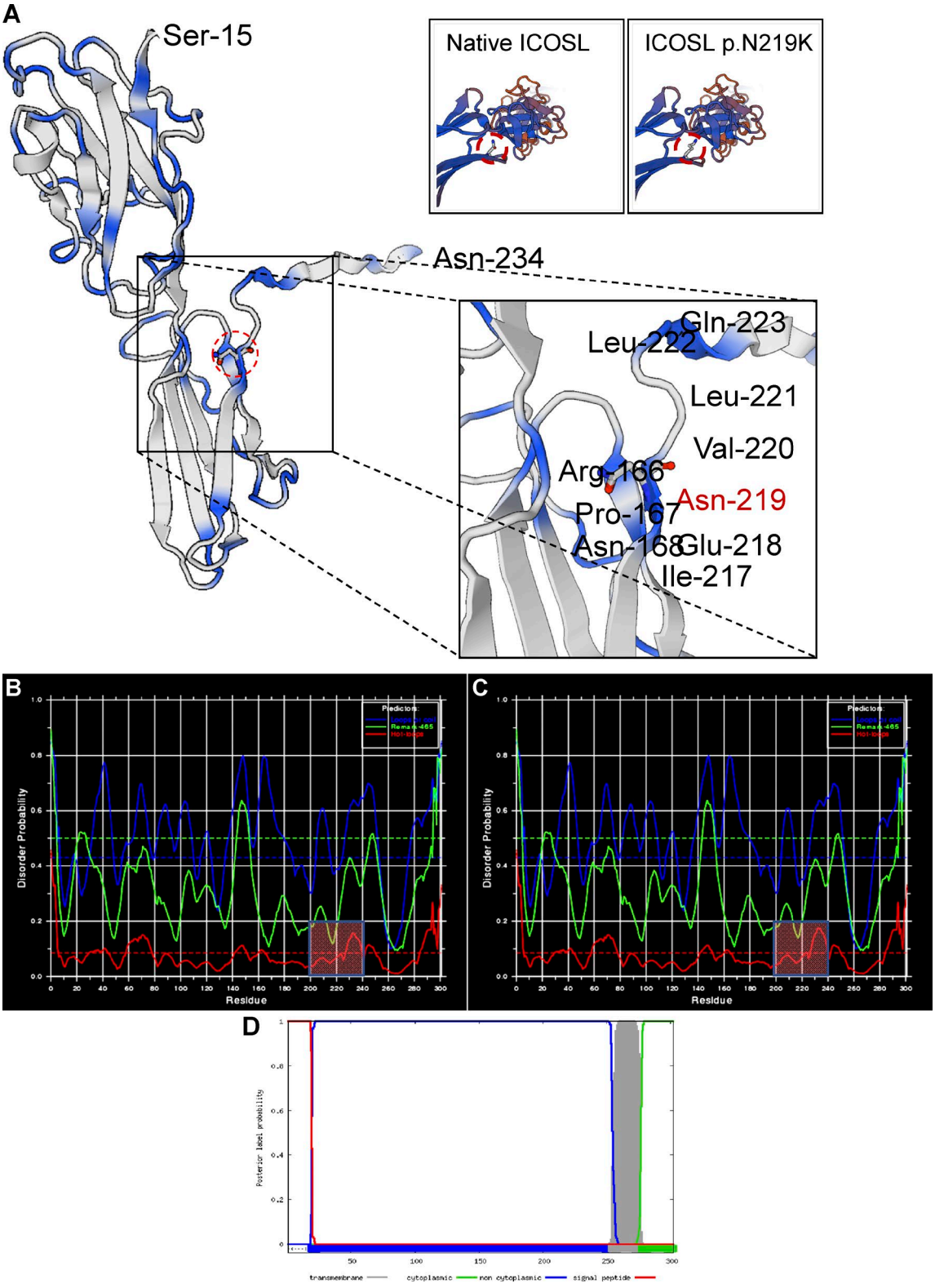

Figure S2. **Homology-predicted 3D structure of ICOSL. (A)** Asn-219 is marked in red (Swiss-Model). The Asn>Lys mutation occurs at a mixed coil-and-strand structure at the protein's extracellular region. **(B–D)** Effect of N219K mutation on ICOSL structural disorder and transmembrane topology. The N219K mutation is predicted to slightly increase disorder probability at the [206–240] region (B to C). It shifts the [206–216] and [226–253] coil structures to [206–215] and [227–253], shortening each region by one amino acid residue. This modification leads to decreased structural stability (i.e., increased disorder probability) and thus lesser molecular rigidity. Although the N219K mutation does not alter the protein's transmembrane topology (D), it renders the molecule more hydrophilic and basic, decreasing its transmembrane stability, potentially explaining its restricted cell-surface expression. Structural disorder prediction was performed by DisEMBL 1.5. Transmembrane topology and protein physicochemical properties were predicted by Phobius and ExPASy, respectively.

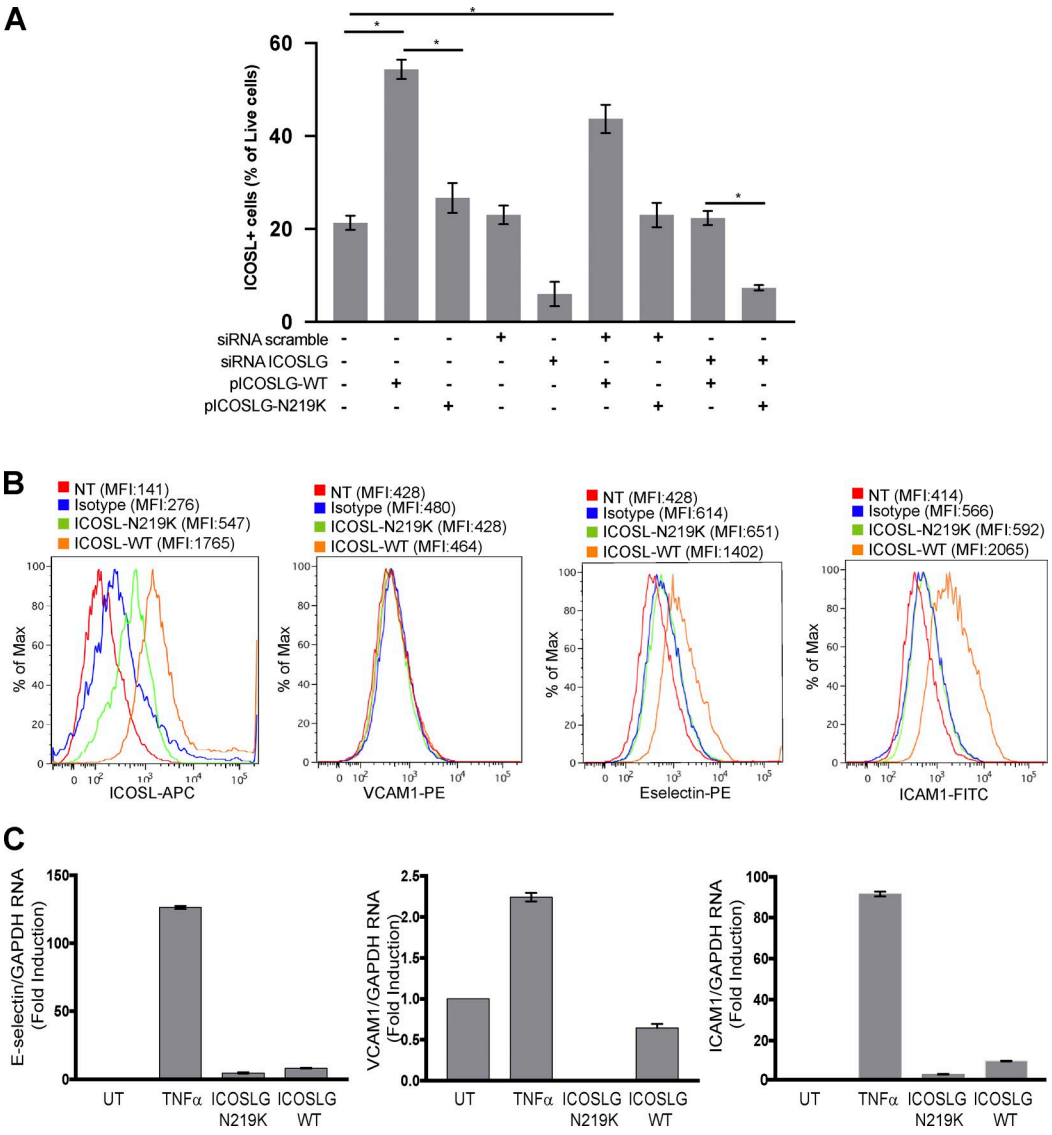

Figure S3. **Silencing of endogenous ICOSL and reconstitution with ICOSL WT or p.N219K.** HMEC-1 cells were silenced for endogenous ICOSL (or scramble control), then transfected with WT or p.N219K ICOSL, and cell-surface expression was evaluated by flow cytometry. **(A)** Percentage of ICOSL$^+$ cells relative to the total number of live cells is depicted. *, $P < 0.05$. **(B)** Analysis of cell-surface expression of ICOSL, VCAM-1, E-selectin, and ICAM-1 on HMEC-1 cells that are either nontransfected (NT) or transfected with ICOSL-WT or ICOSL-N219K. Live-cell gating strategy. MFI, mean fluorescence intensity. **(C)** HMEC-1 were left untreated (UT), pretreated for 2 h with 25 ng/ml TNFα, or transfected with pICOSL-WT or pICOSL-N219K (24 h). The amounts of E-selectin, VCAM-1, and ICAM-1 mRNA were determined by qPCR. Data are representative of three independent experiments.

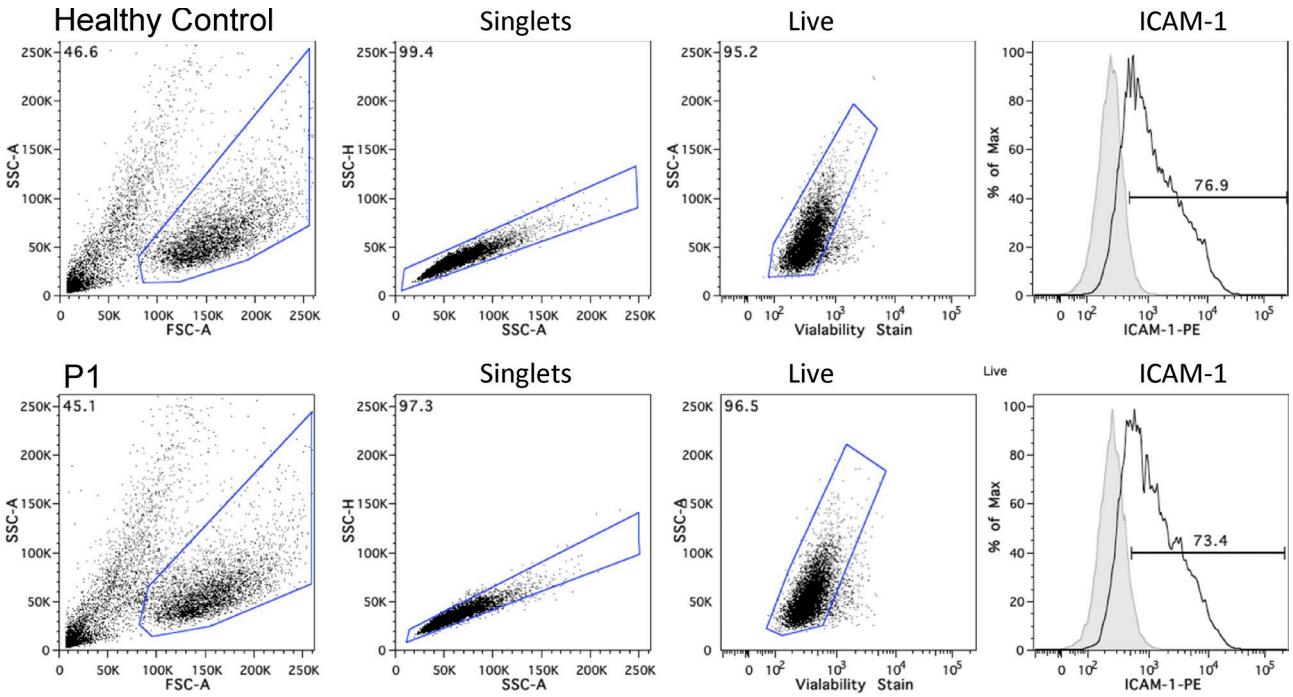

Figure S4. **Identical basal cell-surface expression of ICAM-1 in LCL from HCs and P1.** Flow cytometry analysis of cell-surface expression of ICAM-1 on LCLs. Live-cell gating strategy shown. Histogram demonstrating ICAM-1 expression (dark line) relative to isotype control (shaded). Data are representative of three independent experiments.

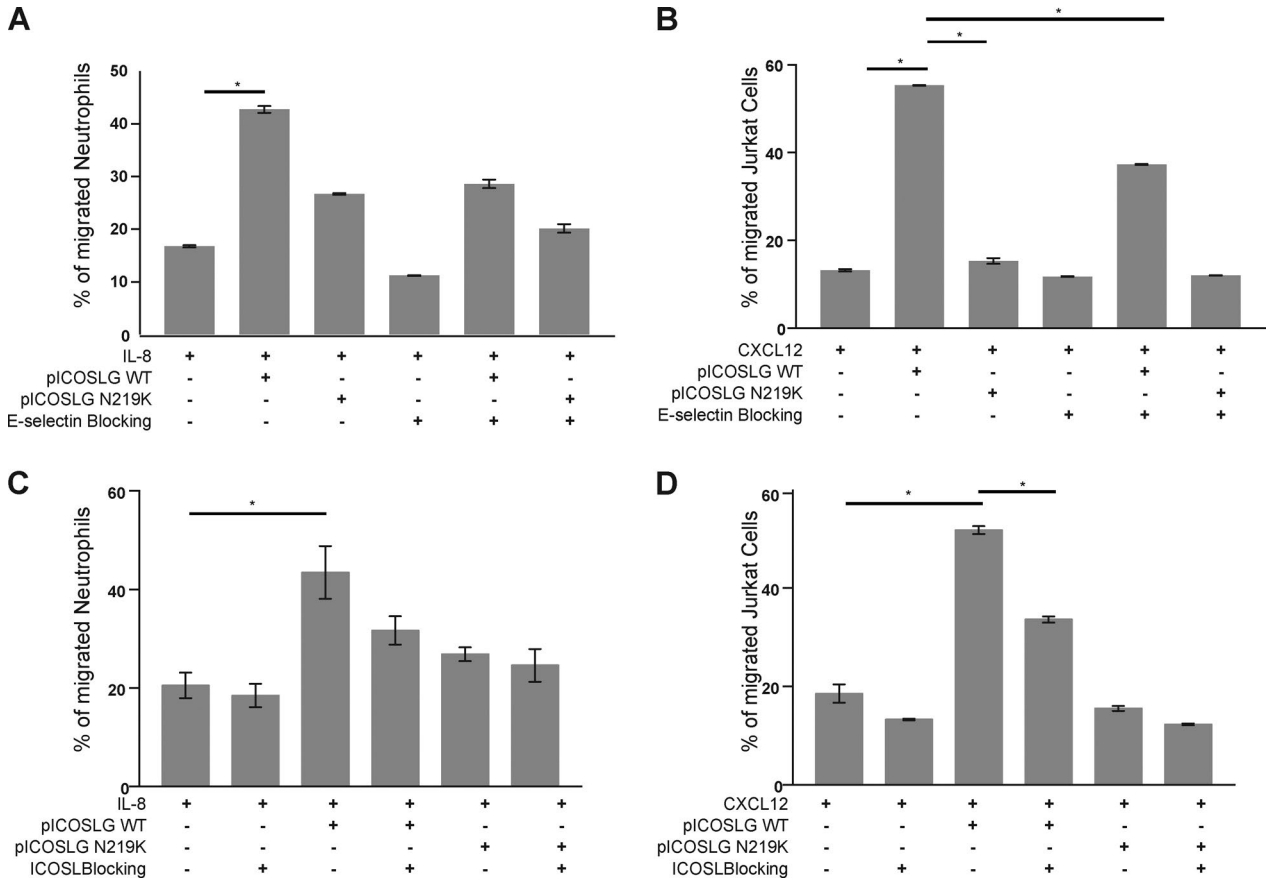

Figure S5. **Contribution of E-selectin and ICOSL to the transendothelial migration of neutrophils. (A–D)** HMEC-1 were reconstituted with pICOSL-WT or pICOSL-N219K for 24 h. E-selectin (A and B) or ICOSL (C and D) were blocked by pretreatment (2 h) with a neutralizing antibody to E-selectin (25 µg/ml) or ICOSL (10 µg/ml), as indicated. Migration of calcein-stained neutrophils to IL-8 (A and C) or Jurkat cells to CXCL12 (B and D) was measured. Results show the percentage of cells that crossed the TNFα-activated endothelial monolayer. Data points represent the means from triplicates, and results are representative of three independent experiments. *, $P < 0.05$.

Table S1 is provided online as an Excel file and contains a list of homozygous and rare non-synonymous heterozygous variants in P1.